Accepted Manuscript

Thiosemicarbazones and 4-thiazolidinones indole-based derivatives: Synthesis, evaluation of antiproliferative activity, cell death mechanisms and topoisomerase inhibition assay

Jamerson Ferreira de Oliveira, Talitha Santos Lima, Débora Barbosa Vendramini-Costa, Sybelle Christianne Batista de Lacerda Pedrosa, Elizabeth Almeida Lafayette, Rosali Maria Ferreira da Silva, Sinara Monica Vitalino de Almeida, Ricardo Olímpio de Moura, Ana Lúcia Tasca Gois Ruiz, João Ernesto de Carvalho, Maria do Carmo Alves de Lima

PII: S0223-5234(17)30384-7

DOI: 10.1016/j.ejmech.2017.05.023

Reference: EJMECH 9453

To appear in: *European Journal of Medicinal Chemistry*

Received Date: 30 January 2017

Revised Date: 4 May 2017

Accepted Date: 6 May 2017

Please cite this article as: J.F. de Oliveira, T.S. Lima, Dé.Barbosa. Vendramini-Costa, S.C.B. de Lacerda Pedrosa, E.A. Lafayette, R.M.F. da Silva, S.M.V. de Almeida, Ricardo.Olí. de Moura, Ana.Lú.Tasca.Gois. Ruiz, Joã.Ernesto. de Carvalho, M.d.C.A. de Lima, Thiosemicarbazones and 4-thiazolidinones indole-based derivatives: Synthesis, evaluation of antiproliferative activity, cell death mechanisms and topoisomerase inhibition assay, *European Journal of Medicinal Chemistry* (2017), doi: 10.1016/j.ejmech.2017.05.023.

Graphical Abstract

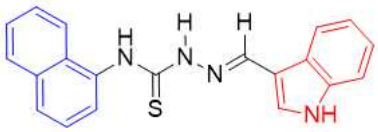

Compound 2b interacts with DNA that has been confirmed by fluorescence suppression

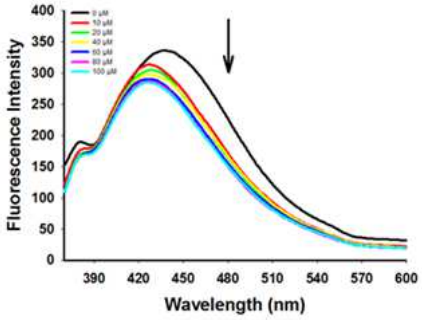

Compound 2b inhibited enzymatic activity of Topo IIα at 50 μM as observed by the formation of topoisomers

HT-29 cells exposed phosphatidylserine residues to the external plasma membrane surface after treatment with compound 2b

Thiosemicarbazones and 4-Thiazolidinones Indole-based derivatives: synthesis, evaluation of antiproliferative activity, cell death mechanisms and topoisomerase inhibition assay

Jamerson Ferreira de Oliveira[a]; Talitha Santos Lima[a]; Débora Barbosa Vendramini-Costa[b,c]; Sybelle Christianne Batista de Lacerda Pedrosa[d]; Elizabeth Almeida Lafayette[e]; Rosali Maria Ferreira da Silva[f]; Sinara Monica Vitalino de Almeida[g]; Ricardo Olímpio de Moura[h]; Ana Lúcia Tasca Gois Ruiz[b]; João Ernesto de Carvalho[b,i]; Maria do Carmo Alves de Lima[a,*]

[a]*Universidade Federal de Pernambuco (UFPE), Departamento de Antibióticos (DANTI), 50670-901, Recife, PE (Brazil)*

[b]*Universidade Estadual de Campinas (Unicamp), Centro Pluridisciplinar de Pesquisas Químicas, Biológicas e Agrícolas (CPQBA) 13083-970, Campinas, SP (Brazil)*

[c] *Cancer Biology, Fox Chase Cancer Center, 19111, Philadelphia, PA (USA)*

[d]*Universidade Federal do Vale do São Francisco (UNIVASF), Colegiado de Ciências Farmacêuticas (CFARM), 56304-205, Petrolina, PE (Brazil)*

[e]*Universidade Federal da Paraíba (UFPB), Departamento de Química e Física (DQF), 58397-000, Areia, PB (Brazil)*

[f]*Universidade Federal de Pernambuco (UFPE), Departamento de Ciências Farmacêuticas (DCFAR), 50670-901, Recife-PE, Brazil*

[g]*Universidade de Pernambuco (UPE), Faculdade de Ciências, Educação e Tecnologia de Garanhuns (FACETEG), 55290-000, Garanhuns-PE, Brazil*

[h]*Universidade Estadual da Paraíba (UEPB), Departamento de Farmácia, 58429-500, Campina Grande, PB (Brazil)*

[i]*Universidade Estadual de Campinas (Unicamp), Faculdade de Ciências Farmacêuticas (FCF), 13083-970, Campinas, SP (Brazil)*

To whom correspondence should be addressed: Maria do Carmo Alves de Lima

[*]Email: nenalima.mariadocarmo@gmail.com

Phone number: +55 8121268347

Fax: +55 8121268346

Abstract

In this study, we report the synthesis and structural characterization of a series of thiosemicarbazone and 4-thiazolidinones derivatives, as well as their *in vitro* antiproliferative activity against eight human tumor cell lines. For the most potent compound further studies were performed evaluating cell death induction, cell cycle profile, ctDNA interaction and topoisomerase IIα inhibition. A synthetic three-step route was established for compounds (**2a-e** and **3a-d**) with yields ranging from 32-95%. Regarding antiproliferative activity, compounds **2a-e** and **3a-d** showed mean GI_{50} values ranging between 1.1 µM (**2b**) - 84.65 µM (**3d**). Compound **2b** was the most promising especially against colorectal adenocarcinoma (HT-29) and leukemia (K562) cells (GI_{50} = 0.01 µM for both cell lines). Mechanism studies demonstrated that 24h-treatment with compound **2b** (5 µM) induced phosphatidylserine residues exposition and G2/M arrest on HT-29 cells. Moreover, **2b** (50 µM) was able to interact with ctDNA and inhibited topoisomerase IIα activity. These results demonstrate the importance of thiosemicarbazone, especially the derivative **2b**, as a promising candidate for anticancer therapy.

Keywords: Medicinal chemistry; anticancer therapy; cellular death; DNA interaction; topoisomerase inhibition

1 Introduction

Cancer remains a major health problem with 14.1 million new cases and 8.2 million deaths by cancer in 2012 worldwide [1]. Although chemotherapy is one of the main therapeutic options for cancer, this form of treatment has limitations such as the possibility of severe adverse effects and the development of resistance. Moreover, as cancer is a group of diseases, there is no specific treatment for some kinds of tumors. In this context, the continuous research and development of new chemical entities is of great relevance for cancer therapy [2].

Among the available cancer therapeutic targets, DNA remains as an attractive target for the development of new drugs that can bind to its structure and artificially alter and/or inhibit its function [3]. Extensive chemical and biochemical studies have characterized a variety of molecules that can react with DNA, conferring various pharmacological effects, such as antibiotic, antitumor, antiviral or antiprotozoal [4]. Once drugs bind to DNA and protein interfaces, the activity of enzymes that metabolize the DNA, such as topoisomerase can be inhibited by the induction of cell death [5].

Topoisomerases are ubiquitous enzymes that alter DNA topology by relieving supercoiling-associated tension in double stranded DNA. These enzymes can perform their function by transiently cutting one strand (type I topoisomerases, Top1) or both DNA strands (type II topoisomerases, Top2) [6]. The ubiquitous presence and crucial biological roles of topoisomerases explain their prevalence as therapeutic target [5]. Moreover, it is widely known that cancer cells possess high levels of topoisomerase activity and show remarkable sensitivity to DNA-targeted drugs [7].

Most clinical drugs that target Top1 or Top2 convert the topoisomerase-associated DNA breaks (known as topoisomerase cleavage complexes) into irreversible DNA damage that initiates the apoptotic program [8]. These topoisomerase-targeted drugs, referred to as topoisomerase poisons, stabilize the topoisomerase cleavage complexes by preventing DNA religation [6]. In addition to their role in the initiation of apoptosis, a growing number of studies show that Top1 and Top2 also participate directly in the execution of the apoptotic program [9]. Since topoisomerase inhibitors can trigger cell death by apoptosis, the elucidation of the relationship between these mechanisms provide opportunities to develop novel therapeutic strategies.

In this context, thiosemicarbazones arise as a promising class of molecules, due to their reported antiproliferative activity in human tumor cell lines [10-12] and associated mechanisms of action, including the ability of interacting with DNA and

topoisomerase inhibition [13-16]. Recent studies in our research group have shown that thiophene-thiosemicarbazone and acridine-thiosemicarbazone derivatives are promising for antitumor activity, presenting the ability to interfere in the cell cycle and to interact with DNA [12,14]. Additionally, the indole nucleus has also been disclosed as a privileged structure in the design of new molecules [17-19].

Continuing our studies with thiosemicarbazone derivatives, this study aimed to synthesize a new series of thiosemicarbazone and 4-thiazolidinones exploring the indole heterocycle. The antiproliferative activity of the new series was evaluated in a panel of eight human tumor cell lines and the most active derivative (compound **2b**) was selected for evaluation of cell death induction, cell cycle profile, DNA interaction and topoisomerase inhibition.

2 Results and Discussion

2.1 Synthesis of thiosemicarbazone and 4-thiazolidinones derivatives

The synthesis of thiosemicarbazone (**2a-e**) and 4-thiazolidinones (**3a-d**) derivatives was performed in three steps (Scheme 1). First, a nucleophilic addition reaction between hydrazine and substituted isothiocyanates afforded a thiosemicarbazide. Then, the synthesized thiosemicarbazides reacted with indole-3-carboxaldehyde, in the presence of a catalytic amount of AcOH, via condensation reaction, leading the thiosemicarbazones [12]. Afterwards, the obtained thiosemicarbazone derivatives were treated with ethyl-2-chloroacetate and sodium acetate affording the respective *N*-3-substituted-4-thiazolidinones [20, 21]. The yields ranged from 32 to 95%

PLEASE INSERT SCHEME 1 HERE

After crystallization, the thiosemicarbazone (**2a-e**) and 4-thiazolidinones (**3a-d**) structures were determined by ^{1}H and ^{13}C NMR, IR and high-resolution mass.

In general, the IR spectrum of thiosemicarbazones **2a-e** displayed stretching of C=N and C=S bonds around 1537-1547 and 1203-1243cm^{-1}, respectively. Thus, the predominance of the thione form of the synthesized thiosemicarbazones was confirmed through the absence of absorption in the 2500-2600 cm^{-1} region [22, 23]. For the 4-thiazolidinones **3a-d**, the IR spectra showed bands at 1398–1362 cm^{-1} characteristic of

NCS bending vibration, providing evidence of ring closure [24, 25]. Finally, the IR spectra of **3a-d** displayed C=O absorbance in the 1701-1722 cm^{-1} region [26].

All the compounds synthesized showed in ^{1}H NMR signals at δ 7.88-7.17 ppm corresponding to protons related to a phenyl group besides a singlet between δ 7.32 and 8.47 ppm attributed to azomethine group (H–C=N), which is in accordance with the reports involving thiosemicarbazones [27, 28]. Moreover, the protons of 4-thiazolidinone ring (S-CH_2) occurred between δ 4.07 and 4.41 ppm [29]. The N–H aromatic (N^4) proton signals appeared at δ 9.50-9.99 ppm region, except for **2d** and **2e**. The presence of a spacer group in N^4 of thiosemicarbazone **2d** and **2e** promoted an electron-releasing inductive effect shifting to downfield region (δ 7.79 and 7.87 ppm, respectively) the N–H aromatic (N^4) proton signals. Finally, the other signals related to thiosemicarbazone, such as N–H hydrazine proton presented chemical shifts at δ 11.49-11.60 ppm region and N–H indole ring showed a singlet peak in the range of δ 11.22 and 11.83 ppm.

Similarly, in the ^{13}C NMR spectra, the chemical shift of azomethine group (H–C=N) appeared at region δ 138.0-153.8 ppm while C=S group occurred in the range δ 174.6-179.8 ppm, both comparable to the literature [30, 31]. The carbon of carbonyl group of 4-thiazolidinone ring occurred between 171.9 and 172.3 δ ppm beside signals in δ 20.64 - 44.9 ppm region attributed to methylene, methyl and spacer groups. In addition, HRMS analysis confirmed the identity of all the synthesized compounds.

The relative configuration (*E* or *Z*) of thiosemicarbazone depends on the aldehyde substituent [32]. For the **2a-e** and **3a-d** series, indole-carboxaldehyde was used. In the ^{1}H NMR spectrum analysis, it was possible to detect a single peak, referring to a chemical shift of 7.32 to 8.47 δ ppm for the singlet azomethine hydrogen. Furthermore, it was also observed in our experiments the appearance of a single spot in thin layer chromatography (TLC), indicating the presence of a single isomeric form.

In this study, compound **2b**, the most promising compound in the series, was chosen for elucidation of isomerism of the derivatives synthetized. Thus, in 2D NMR NOESY spectrum, it was observed the spatial correlation between the hydrogen of =N-NH- at δ 11.68 ppm and azomethine (-CH=N-) at δ 8.49 ppm, as well as no spatial interaction between the hydrogen in position 2 of the indole (-CH=C-) at δ 7.92 ppm and the hydrogen azomethine (-CH=N-) at δ 8.47 ppm m (See supplementary material). These results suggested the *E* configuration, which corroborates the crystallographic

studies of X-ray and NOESY spectrum of *E*-thiosemicarbazone presented in the literature [12, 33].

2.1 Evaluation of the antiproliferative activity in human tumor cell lines

Considering that different cell lines display different sensitivities toward the same cytotoxic compound, the antiproliferative activity of thiosemicarbazone (**2a-e**) and 4-thiazolidinones (**3a-d**) were evaluated *in vitro* against eight different human cancer cell lines [U251 (glioma), MCF-7 (breast), NCI-ADR/RES (multidrug resistant ovary carcinoma), 786-0 (renal), NCI-H460 (non-small cell lung cancer), OVCAR-3 (ovary), HT-29 (colon), and K-562 (leukemia)] according to the National Cancer Institute of United States protocols (NCI-US) [34]. The antiproliferative activity of each compound was also evaluated *in vitro* against spontaneously transformed keratinocytes from histologically normal skin (HaCat cells). Doxorubicin was employed as the positive control [35].

The antiproliferative activity was represented as the GI_{50} (concentration of compound that inhibits 50% of cell growth, Table 1) and the mean values ranged between 1.1 µM (compound **2b**) and 84.65 µM (compound **3d**). Based on this mean values expressed as logarithm, Fouche et al. (2008) [36] described four levels of activity named inactive (mean log $GI_{50} > 1.50$), weak activity ($1.50 \geq$ mean log $GI_{50} > 1.10$), moderate activity ($1.10 >$ mean log $GI_{50} > 0$) and potent activity (mean log $GI_{50} < 0$). Considering these criteria, compounds **2e** and **3a-d** were considered inactive while **2a**, **2c** and **2d** showed a moderate activity besides **2b** that presented a potent antiproliferative activity (Table 1).

These results suggest that transforming thiosemicarbazone **2a-d** into *N*-3-substituted-4-thiazolidinones **3a-d** by a non-classical bioisosteric modification resulted in lack of antiproliferative effects (Table 1). Between thiosemicarbazone derivatives, the absence of bromine in the indole ring associated to the 1-naphthyl group connected to N^4 (**2b**) resulted in better antiproliferative activity (mean log GI_{50} = -0.69, potent activity) with selectivity against colorectal adenocarcinoma (HT-29) and leukemia (K562) cell lines (GI_{50} = 0.01 µM, for both cell lines). The substitution of the naphthyl group (**2b**) for the p-toluyl (**2c**) or 2-phenethyl (**2e**) resulted in moderate (mean log GI_{50} = 0.39) to inactive (mean log $GI_{50} > 1.47$) results, respectively (Table 1).

The strategy for the design of derivatives in this study was based on previous studies by our research group [12,14]. The best compounds evaluated by Oliveira et al.

(2015) and Almeida et al. (2015) presented mean log GI_{50} of 0.75 and 0.88, respectively, characterizing these compounds as being of moderate activity. Our proposal for molecular modification of thiophene and acridine heterocycles by the heteroaromatic nucleus of indole increased substantially antiproliferative activity (mean log GI_{50} = -0.69).

The introduction of an aliphatic spacer group between N^4-thiosemicarbazone and the phenyl ring, as found in **2d** and **2e**, did not exert a positive effect on the cytostatic activity. Oliveira et al. (2015) [12] described that this kind of substitution did not improve the cytostatic activity of 2-thiophene-thiosemicarbazone derivatives. Moreover, the presence of a bromine in the indole ring (**2d**) improved the antiproliferative activity of the 2-phenethyl thiosemicarbazone derivatives. Thus, while **2e** was inactive, **2d** showed a moderate antiproliferative activity (Table 1).

Therefore, the presence of an aromatic group at N^4 seemed to be the main factor for the biological activity displayed by this series of compounds (**2a-e**) while the substitution in the indole nucleus of thiosemicarbazones afforded a secondary contribution.

In order to simulate the behavior of compounds against normal cells, the HaCat cell line (immortalized human keratinocyte) was inserted into the evaluation panel. Inactive compounds (**2e**, **3b**, **3c** and **3d**) were shown to be non-cytotoxic. On the other hand, the most potent compound of the series (**2b**), also presented cytostatic effect in this lineage (GI_{50} = 0.50 μM). However, the results presented *in vitro* cytotoxicity do not necessarily have repercussions on *in vivo* toxicity assays. Oliveira et al. (2015) [12] chose, in their antiproliferative *in vitro* study, a potent compound against tumor cells that was also cytotoxic in the HaCat lineage. Subsequently, the acute toxicity of this compound was evaluated, in which no severe clinical side effects were observed.

PLEASE INSERT TABLE 1 HERE

2.2 Cell Cycle and Cell Death Analyses of Compound 2b

Based on antiproliferative activity (Table 1), compound **2b** was chosen for analyses of cell cycle and cell death on colorectal adenocarcinoma cell line (HT-29, GI_{50} = 0.01 μM, Table 1). In the first set of experiments, the induction of phosphatidylserine (PS) exposure was evaluated by the ability of annexin-V to bind PS

residues translocated to the outer face of the cell membrane during the early stage of cell death, while 7-AAD binds to the DNA only after loss of cell membrane integrity.

After 24h, compound **2b** reduced HT29 cells viability (unstained cells) in a concentration-dependent manner and increased double stained cell subpopulations (PS residues exposition along with lack of cell membrane integrity) and 7-AAD stained (only lack of cell membrane integrity) in a similar profile. Only at the lowest concentration (5 μM), **2b** increased (12.6 ± 1.6 %) the cell subpopulation with PS residues exposition without lack of membrane integrity (Figure 1). These data suggested that compound **2b** induces cell death in a concentration-dependent way, possibly through externalizing phosphatidylserine residues prior to membrane integrity lack.

PLEASE INSERT FIGURE 1 HERE

Furthermore, **2b** (5, 10 and 30 μM) induced G2/M arrest, more pronouncedly in smaller concentrations, followed by a decrease in G1- and S-phase populations (Table 2). These results were similar to those obtained for colchicine (1.25 nM, positive control), a natural product that binds to tubulin leading microtubule destabilization and prevents mitosis progress [37]. Moreover, the induction of G2/M arrest by microtubule-targeting agents can be followed by induction of programmed cell death process [38]. Consequently, the promotion of cell cycle arrest in G2/M phase by **2b** (Table 2) can induce programmed cell death process initialized by PS residues externalization (Figure 1).

PLEASE INSERT TABLE 2 HERE

One of the features of cancer cells is presenting sustained proliferative capacity, which favors the propagation of mutations and contributes to genetic instability, one of the characteristics of tumorigenesis [39]. Thus, therapies that interfere and limit this capacity are desirable, to which compound **2b** has proved to be a promising alternative.

2.3 DNA binding properties of compound 2b

Indole derivative biological activities have been associated to DNA binding power and correlated to apoptosis of cancer cells since this type of death can be

attributed to the alteration of nucleic acid structure, function or stability [40]. Moreover, interaction between indole compounds and specific regions of nucleic acid can modulate several key cell processes as DNA replication [41].

Aiming to understand the means by which **2b** exerts G2/M arrest on HT-29 cells, the mode of interaction of **2b** with DNA was evaluated. Generally, small organic compounds can interact to DNA by intercalation, DNA-groove binding or by attractive electrostatic interactions [42]. Monitoring UV-Visible absorption in Tris-HCl buffer (10 mM, pH 7.6), **2b** showed maximum absorption peak at 334 nm and calf thymus DNA (ctDNA) did not demonstrate absorption at the same λ, when they were analyzed separately. Titration of increasing amounts of ctDNA into **2b** solution led to increased absorption (hyperchromic effect), presenting hyperchromicity of 13 % at 100 µM of ctDNA. Both hyperchromic and hypochromic effects are characteristic of conformational alterations of the DNA double helix after compound binding [43]. Generally, hypochromism combined with a redshift is considered an indicative of intercalation of small molecules to the DNA due to the stacking of the chromophore pairs [3, 14, 44]. Besides, the hyperchromic effect suggests changes on DNA conformation and structure (denaturation) [4, 45]. Therefore, the UV-Visible absorption result suggested that **2b** promoted changes on DNA conformation.

Using the model proposed by McGhee and Von Hippel (1974) [46] the binding constant value (Kb) of **2b** was estimated in 4.3 x 10^4 M^{-1} (Table 3). Binding constant values in the range of 10^4 are typical of complexes formed between DNA and organic dyes [42], indicating moderate binding to DNA [47].

PLEASE INSERT TABLE 3 HERE

The positive influence of hydrogen donor groups on ctDNA binding affinity is observed in several studies [48-50]. Here, the presence of NH groups in the hydrazine-carbothioamide portion of **2b** could contribute to ctDNA binding ability. Janardan et al. (2014) [51] have synthesized hydrazine and semicarbazide derivatives with DNA binding properties confirmed by UV-Vis and IR techniques. For both intercalation and groove bind, DNA and organic compound interactions occur by hydrogens and Van der Waals bonds [52]. Compounds bearing typical aromatic rings such as pyrrole, furan or benzene as lateral chain with torsional freedom, can bind to the DNA groove producing little or no structural rearrangement of the DNA helix, unlike intercalators [4, 53].

Almeida et al (2015) [14] showed that derivative 2-(acridin-9-ylmethylene)-*N*-(naphtalen-1-yl)-hydrazinecarbothioamide intercalates DNA with a binding constant value of 8.47 x 10^5 M^{-1}. The presence of the naphthlen ring and hydrazine-carbothioamide group strengthens their interaction with DNA. In addition, acridine ring is the structural difference compared to derivative **2b** and confirms the importance of planarity of the aromatic ring in the increased affinity to DNA [54].

Moreover, fluorescence spectroscopy was used to confirm the interaction between **2b** and ctDNA, since fluorescence quenching studies can give some information on the binding of small molecules to biomacromolecules on the molecular level [55, 56]. Fluorescence spectra of **2b** (15 μM; $\lambda_{excitation}$ 335 nm; $\lambda_{emission}$ 435 nm) were monitored in the absence and presence of increasing amounts of ctDNA (0-100 μM) demonstrating that increases in ctDNA concentration promoted decrease on **2b** fluorescence emission (Figure 2). Suppression in fluorescence intensity in the presence of DNA can be observed when groove binding agents [57, 58], electrostatic [59], hydrogen bonding [60] or hydrophobic interactions are involved [61].

Quantitative analysis of fluorescence quenching was determined from the plot of the relative intensity of fluorescence versus the concentration of ctDNA, and the fluorescence suppression constant (Ksv) was obtained using the Stern-Volmer equation [62]. Derivative **2b** presented a Ksv value of 1.19 x 10^3 M^{-1}, indicating the interaction with ctDNA [3]. Emission-quenching phenomena reflect the interaction between the derivative and ctDNA, consistent with the electronic absorption spectroscopy results [63]. Both Ksv and Kb constants of the derivative **2b** indicate static quenching due to complex formation between the new derivative and ctDNA. Moreover, the reduction of fluorescence emission by derivative **2b** was accompanied by an apparent change in the maximum wavelength of fluorescence emission, with a shift of 8 nm that is indicative of a physical interaction with ctDNA [64]. These DNA-binding results could explain the cell cycle arrest and the topoisomerase-DNA interface interaction that were evaluated by topo IIα inhibition assay and that can be related to apoptosis pathway.

PLEASE INSERT FIGURE 2 HERE

2.4 Topoisomerase IIα assay

Topoisomerase (Topo) inhibitors are molecules that impair the enzymatic activity by forming of a ternary complex (DNA-Topo-compound) or by catalytic

inhibition, resulting in cell death by apoptosis [9, 65, 66]. Some antitumor drugs already used in clinical practice have topoisomerase as biological target, such as doxorubicin and daunorubicin (anthracycline group), etoposide and teniposide (epipodophyllotoxins group), amsacrine (acridines group) and some thiosemicarbazones [67, 68]. However, these drugs present many side effects, which prompts the development of new topoisomerase inhibitors [69].

Among the mammalian topoisomerases, Topo IIα is preferentially expressed in proliferating cells consisting in an important target for the discovery of new antitumor drugs [8]. Compound **2b** was evaluated in the DNA plasmid relaxation assay. This assay consisted in the evaluation of topo IIα enzymatic activity in the absence and presence of the compound followed by electrophoresis analysis [70]. As demonstrated in Figure 3, the circular plasmid pUC19 can exist in three different topological conformations: supercoiled circular DNA, nicked circular DNA and linear DNA, all of which have identical sequences, but migrate at different rates through agarose gel. Owing to their compact nature, supercoiled DNA topoisomers migrate faster through agarose in comparison to linear DNA, nicked circular DNA, or relaxed DNA. When topo IIα is active, the plasmid migrates as a single band and much more slowly. On the other hand, inhibition of topo IIα results in a similar band pattern compared to plasmid DNA (first lane). The activity of **2b** as topo II inhibitor was visualized by the formation of topoisomers for both tested concentration, but the inhibition was partial when compared to the positive control used (*m*-AMSA).

PLEASE INSERT FIGURE 3 HERE

The topo II inhibition probably corroborates other mechanisms of action identified in this work, such as cell cycle arrest and phosphatidylserine residues exposition to the external plasma membrane surface. The formation of DNA topoisomers indicates that the cleavage complex was stabilized which could be due to alkylation of the thiol residues in the DNA-topo II complex by the thiosemicarbazone moiety [71].

Indole derivatives are also known for their inhibitory activity against topo II. Some indenoindolone-thiosemicarbazones were synthesized and evaluated for their potential in inhibiting topo II. Kashyap et al. (2013) in their study evaluated the capacity of inhibition of topoisomerase of indeneindolones. It was found that two derivatives of

the series could inhibit the enzyme activity, without DNA intercalation [72]. In this way, this pharmacophore may also have contributed to the biological action of derivative **2b**.

It is worthwhile to highlight that there is a relationship between inhibition of topo II and cell cycle arrest. Recent studies show that the cell cycle arrest observed in cancer cells treated with topo II poisons is primarily in the G2/M phase [73]. These data corroborate our results, where the compound **2b** could cause arrest at the G2/M phase of the cell cycle. This suggests indole-thiosemicarbazone derivative, in particular compound **2b**, as candidate for anticancer therapy.

3 Conclusions

This study showed the antiproliferative activity of thiosemicarbazones and 4-thiazolidinones indole-based derivatives, with emphasis on derivative **2b** that presents important chemical characteristics such as the presence of the indole, thiosemicarbazone and naphthalene moieties. As far as our results have suggest, **2b** can interact with DNA and inhibit topo IIα that probably could explain PS residues externalization and G2/M arrest in HT-29 cells highlighting as a promising candidate for use in anticancer therapy.

4 Experimental Section

4.1 Chemistry

All reagents used in this study are commercially available (Sigma-Aldrich, Acros Organics, Vetec). The melting points were determined on Quimis 340 (Quimis, Brazil) apparatus and are uncorrected. IR spectra were measured on Bruker IFS-66 IR spectrophotometer (Bruker, Germany) using KBr pellets. NMR spectra were recorded on Varian UnityPlus spectrometer 400 MHz (400 MHz for ^{1}H and 100 MHz for ^{13}C) or a Bruker AMX-300 MHz (300 MHz for ^{1}H and 75.5 MHz for ^{13}C) instruments by using tetramethylsilane as an internal standard. DMSO-d_6 was purchased from Sigma-Aldrich. HRMS were performed on a MALDI-TOF Autoflex III (Bruker Daltonics, Billerica, MA, USA). The chemical shifts were reported in δ units, and coupling constants (*J*) were reported in Hertz (Hz). The multiplicities were given as s (singlet), d (doublet), t (triplet), m (multiplet), dd (double doublet). TLC development was conducted on 0.25 mm silica gel plates (Merck, silica gel 60 F_{254} in aluminium foil).

4.1.2 General procedure for compounds 2a-e

Substituted thiosemicarbazide (1 mmol) and 3-5 drops of acetic acid were added to a solution of indole-3-carboxaldehyde (1 mmol) in ethanol (10 mL). The reaction was processed under magnetic stirring for 2h at room temperature. The precipitate was filtered off, washed with ethanol then dried in desiccator under vacuum. Additional amount of desired compound could be recovered from the filtrate after cooling. After drying, the product was recrystallized from ethanol [12].

4.1.2.1 (E)-2-(5-bromo-1H-indol-3-ylmethylene)-N-(naphthalen-1yl)hydrazinecarbothioamide (2a)

White powder; MP: 205-207°C; Yield: 77%; Rf: 0.54 ($CHCl_3$/MeOH 9.5:0.5) NMR ^1H (300 MHz, DMSO) δ: 7.33 (m, 1H, indole), 7.41 (s, 1H, indole), 8.46 (s, 2H, indole), 8.00 (s, 1H, =CH-), 8.00-7.43 (m, 7H, naphtyl), 9.99 (s, 1H, NH), 11.69 (s, 1H, NH), 11.88 (s, 1H, NH). NMR ^{13}C (75 MHz, DMSO) δ: 110.73, 113.38, 113.86, 122.69, 123.88, 125.31, 125.31, 125.68, 125.68, 125.99, 126.26, 126.42, 128.09, 130.13, 132.53, 133.65, 135.42, 135.80, 140.98, 176.21. IR (KBr, cm^{-1}): 3320.50 (NH), 3200.00 (NH), 3164.90 (NH), 750.00 (CS). HRMS *m/z* $[M + H]^+$ calcd for $C_{20}H_{15}BrN_4S$: 422.0201; found: 423.3289.

4.1.2.2 (E)-2-(1H-indol-3ylmethylene)-N-(naphthalen-1-yl)hydrazinecarbothioamide (2b)

White powder; MP: 185-187°C; Yield: 95%; Rf: 0.44 ($CHCl_3$/MeOH 9:1). NMR ^1H (300 MHz, DMSO) δ: 7.09 (t, 1H, J= 7.5Hz, indole), 7.20 (t, 1H, J= 7.5Hz, indole), 7.46 (d, 1H, J= 8.1Hz, naphtyl), 7.63-7.51 (m, 3H, naphtyl), 7.69 (d, 1H, J= 7.2Hz, indole), 7.89 (d, 1H, J= 8.2Hz, napthyl), 7.93 (d, 1H, J= 2.7Hz, indole), 8.03-7.95 (m, 2H, naphtyl), 8.37 (d, 1H, J= 7.9 Hz, indole), 8.51 (s, 1H, =CH-), 9.87 (s, 1H, NH), 11.69 (s, 2H, NH). NMR ^{13}C (75 MHz, DMSO) δ: 111.07, 111.75, 120.55, 122.17, 122.64, 122.92, 124.01, 125.40, 125.88, 125.97, 126.08, 126.51, 128.06, 130.38, 131.38, 133.68, 135.70, 137.06, 141.34, 176.22. IR (KBr, cm^{-1}): 3319.51 (NH), 3158.5 (NH), 773.75 (CS) HRMS *m/z* $[M + H]^+$ calcd for $C_{20}H_{16}N_4S$: 344.1096; found: 344.4328.

4.1.2.3 (E)-2-(1H-indol-3-ylmethylene)-N-(p-toluyl)hydrazinecarbothioamide (2c)

White powder; MP: 195-197°C; Yield: 32%; Rf: 0.55 ($CHCl_3$/MeOH 9:1). NMR ^1H (300 MHz, DMSO) δ: 3.43 (s, 3H, CH_3), 7.17 (d, 2H, J= 8.1Hz, fenil), 7.48 (d, 2H, J= 8.4Hz, phenyl), 7.23-7.11 (m, 2H, indole), 7.44 (d, 1H, J= 7.5Hz, indole), 7.88 (d, 1H,

J= 2.7Hz, indole), 8.20 (d, 1H, J= 7.5Hz, indole), 8.39 (s, 1H, =CH-), 9.50 (s, 1H, NH), 11.49 (s, 1H, NH), 11.66 (s, 1H, NH). NMR ^{13}C (DMSO, 75MHz) δ: 20.64, 111.03, 111.98, 120.79, 121.83, 122.77, 124.13, 125.19, 125.19, 128.70, 128.70, 131.29, 134.26, 136.74, 137.11, 141.23, 174.62. IR (KBr, cm^{-1}): 3409.4 (NH), 3314.1 (NH), 3164.9 (NH), 744.1 (CS). HRMS *m/z* $[M + H]^+$ calcd for $C_{17}H_{16}N_4S$: 308.1096; found: 308.4007.

4.1.2.4 (E)-2-((5-bromo-1H-indol-3-yl)methylene)-N-phenethylhydrazinecarbothio-amide (2d)

White powder; MP: 220-222°C; Yield: 86%; Rf: 0.46 ($CHCl_3$/MeOH 9:1). NMR ^{1}H (300 MHz, DMSO) δ: 2.38 (t, 2H, J= 6.9Hz, CH_2), 3.82 (m, 2H, J= 5.7Hz, CH_2), 7.21-7.17 (m, 1H, indole), 7.43-7.40 (m, 1H, indole), 7.98 (d, 1H, J= 2.4Hz, indole), 8.27 (d, 1H, J= 3.9Hz, indole), 7.35-7.21(m, 5H, phenyl), 7.87 (d, 1H, J= 5.4Hz, NH), 8.25 (s, 1H, =CH-), 11.25 (d, 1H, J= 3Hz, NH), 11.81 (s, 1H, NH). NMR ^{13}C (75 MHz, DMSO) δ: 34.82, 44.98, 110.75, 113.34, 113.89, 123.67, 125.31, 125.57, 126.18, 128.44, 128.44, 128.56, 128.56, 132.07, 135.76, 139.26, 140.13, 176.09 (CS). IR (KBr, cm^{-1}): 3420.25 (NH), 3365.13 (NH), 3200.00 (NH), 1737.84 (CS). HRMS *m/z* $[M + H]^+$ calcd for $C_{18}H_{17}BrN_4S$: 400.0357; found: 401.3234.

4.1.2.5 (E)-2-((1H-indol-3-yl)methylene)-N-phenethylhydrazinecarbothioamide (2e)

White powder; MP: 197-199°C; Yield: 73%; Rf: 0.51 ($CHCl_3$/MeOH 9:1). NMR ^{1}H (300 MHz, DMSO) δ: 2.95 (t, 2H, J= 7.8Hz, CH_2), 3.85 (quart., 2H, J= 7.2Hz, CH_2), 7.15-7.10 (m, 1H, indole), 7.42 (d, 1H, J= 8.1Hz, indole), 7.39-7.18 (m, 5H, phenyl), 7.79 (d, 1H, J= 2.7Hz, NH), 7.84 (d, 1H, indole, J=7.8Hz), 7.98 (d, 1H, indole, J=5.4Hz), 8.28 (s, 1H, =CH), 11.22 (s, 1H, NH), 11.60 (s, 1H, NH). NMR ^{13}C (75 MHz, DMSO) δ: 34.88, 44.71, 111.03, 111.76, 120.57, 121.83, 122.60, 123.82, 126.20, 128.47, 128.47, 128.57, 128.57, 131.06, 137.04, 139.27, 140.68, 175.84 (CS). IR (KBr, cm^{-1}): 3365.00 (NH), 3256.37 (NH), 3200.00 (NH), 746.08 (CS). HRMS *m/z* $[M + H]^+$ calcd for $C_{18}H_{18}N_4S$: 322.1252; found: 322.4273.

4.1.3 General procedure for compounds 3a-d

A solution of 1 mmol of thiosemicarbazones, 1.1 mmol of ethyl-2-chloroacetate, and 4 mmol of sodium acetate anhydrous in 20 mL of ethanol was stirred until reflux to the completion of the reaction (16-24 h). After, the solution was cooled to 0º C, the

precipitate was collected with filter under vacuum and washed with hot methanol and water [20,21].

4.1.3.1 (E)-2-(E)-(5-bromo-1H-indol-3ylmethylene)hydrazono)-3-(naphthalen-1 yl)thiazolidin-4-one (3a)

White powder; MP: 280-282°C; Yield: 35%; Rf: 0.58 ($CHCl_3$/MeOH 9:1). NMR ^1H (300 MHz, DMSO) δ: 4.41-4.33 (m, 2H, CH_2), 7.32 (m, 1H, indole), 7.35 (m, 1H, indole), 8.24 (m, 1H, indole), 8.40 (m, 1H, indole), 7.42 (m, 1H, naphtyl), 7.76-7.57 (m, 5H, naphtyl), 8.07 (m, 1H, naphtyl), 8.07 (s, 1H, =CH-), 11.79 (s, 1H, NH). IR (KBr, cm^{-1}): 3345.7 (NH), 3053.8 (NH), 2977.5 (NH), 1707.48 (CO). HRMS *m/z* $[M + H]^+$ calcd for $C_{22}H_{15}BrN_4OS$: 462.0150; found: 463.3497.

4.1.3.2 (E)-2-(E)-(1H-indol-3-ylmethylene)hydrazono)-3-(naphthalen-1-yl)thiazolidin-4-one (3b)

White powder; MP: 265-267°C; Yield: 45%; Rf: 0.59 ($CHCl_3$/MeOH 9.5:0.5). NMR ^1H (300 MHz, DMSO) δ: 4.35 (d, 1H, J= 17.1Hz, CH_2), 4.19 (d, 1H, J= 16.2Hz, CH_2), 7.20 (m, 2H, indole), 8.08 (d, 1H, J= 8.1Hz, indole), 8.23 (d, 1H, J= 8.4Hz, indole), 7.44 (m, 1H, naphtyl), 7.69-7.58 (m, 5H, naphtyl), 7.79-7.76 (m, 1H, naphtyl), 8.27 (s, 1H, =CH), 11.62 (s, 1H, NH). NMR ^{13}C (75 MHz, DMSO) δ: 32.40, 111.75, 111.98, 120.79, 121.95, 122.46, 122.69, 124.42, 125.83, 126.52, 127.13, 127.13, 128.34, 129.37, 129.37, 132.01, 132.01, 133.91, 137.10, 153.89, 161.51, 172.32 (CO). IR (KBr, cm^{-1}): 3394.93 (NH), 1613.64 (CO). HRMS *m/z* $[M + H]^+$ calcd for $C_{22}H_{16}N_4OS$: 384.1045; found: 384.4536.

4.1.3.3 (E)-2-(E)-(5-bromo-1H-indol-3-ylmethylene)hydrazono)-3-(p-toluyl)thiazolidin-4-one (3c)

White powder; MP: 295°C; Yield: 32%; Rf: 0.56 ($CHCl_3$/MeOH 9.5:0.5). NMR ^1H (300 MHz, DMSO) δ: 2.37 (s, 3H, CH_3), 4.11 (s, 2H, CH_2), 7.28 (d, 2H, J= 8.7Hz, phenyl), 7.43 (d, 2H, J= 8.7Hz, phenyl), 7.35-7.24 (d, 2H, indole), 8.40 (m, 2H, indole), 7.82 (s, 1H, =CH-), 11.83 (s, 1H, NH). NMR ^{13}C (75 MHz, DMSO) δ: 111.42, 113.45, 114.01, 125.17, 127.93, 127.93, 127.93, 127.93, 129.49, 129.49, 129.49, 129.49, 132.58, 133.10, 135.78, 135.78, 138.05, 153.22, 171.98 (CO). IR (KBr, cm^{-1}): 3255.75 (NH), 1608.29 (CO). HRMS *m/z* $[M + H]^+$ calcd for $C_{19}H_{15}BrN_4OS$: 426.0150; found: 427.3176.

4.1.3.4 (E)-2-(E)-(1H-indol-3ylmethylene)hydrazono)-3-(p-toluyl)thiazolidin-4-one (3d)
White powder; MP: 274-276°C; Yield: 72%; Rf: 0.57 ($CHCl_3$/MeOH 9.5:0.5). NMR ^1H (300 MHz, DMSO) δ: 2.38 (s, 3H, CH_3), 4.07 (s, 2H, CH_2), 7.25 (d, 2H, J= 8.4Hz, phenyl), 7.32 (d, 2H, J= 8.4Hz, phenyl), 7.21-7.14 (m, 1H, indole), 7.45 (d, 1H, J= 6.6Hz, indole), 7.77 (d, 1H, J= 2.4Hz, indole), 8.22 (d, 1H, J= 6.6Hz, indole), 8.42 (s, 1H, =CH-), 11.64 (s, 1H, NH). NMR ^{13}C (DMSO, 75MHz) δ: 32.14, 120.77, 122.69, 124.47, 127.96, 127.96, 127.96, 127.96, 129.49, 129.49, 129.49, 129.49, 132.01, 132.64, 137.11, 138.02, 153.70, 154.49, 172.00 (CO). IR (KBr, cm^{-1}): 3405.71 (NH), 1722.24 (CO). HRMS *m/z* $[M + H]^+$ calcd for $C_{19}H_{16}N_4OS$: 348.1045; found: 348.4215.

4.2 Biological Assay

4.2.1 Cell culture conditions

Eight different human cancer cell lines [U251 (glioma), MCF-7 (breast), NCI-ADR/RES (multidrug resistant ovary carcinoma), 786-0 (renal), NCI-H460 (non-small cell lung cancer), OVCAR-3 (ovary), HT-29 (colon), and K-562 (leukemia)] were kindly provided by National Cancer Institute at Frederick (NCI-USA). The immortalized human keratinocyte (HaCaT) cell line was kindly provided by prof. Dr. Ricardo Della Coletta (University of Campinas). All cell lines were maintained in RPMI 1640 (Gibco, USA) supplemented with 5% (v/v) fetal bovine serum (FBS, Gibco) and 1% (v/v) penicillin:streptomycin (Nutricell, 1000 U/mL:1000 g/mL) in a humidified atmosphere with 5% CO_2, at 37°C. For the experiments, HaCaT and CHO-K1 were used between passages 5 to 12.

4.2.2 Samples preparations

Compounds **2a-e** and **3a-d** (5 mg) were initially diluted in DMSO (50 µl) followed by the addition of 950 µL of RPMI 1640/FBS 5% (working solution). Final concentrations (0.25, 2.5, 25 and 250 µg/mL, for antiproliferative assay; 5, 10, 20, 30 and 50 µM, for flow cytometry experiments of **2b**) were obtained by serial dilution in RPMI 1640/FBS 5%. Doxorubicine (0.025, 0.25, 2.5 and 25 µg/mL, final concentration) and Colchicine (1.25nM, final concentration) were used as positive controls on antiproliferative and cell cycle assays, respectively.

4.2.3 Antiproliferative assay

The *in vitro* antiproliferative activity assay was performed as described by Monks et al. (1991) [74]. Each cell line was plated in 96-well plates (100 µL cells/well) for 24h and then exposed to the derivatives **2a-e** and **3a-d** in different concentrations at 37º C, 5% of CO_2 in air for 48 hours. Final DMSO concentration (< 0,25%) did not affect cell viability. Before (T_0 plate) and after (T_1 plates) sample addition, cells were fixed with 50% trichloroacetic acid and cell proliferation determined by spectrophotometric quantification (540 nm) of cellular protein content using sulforhodamine B assay. The GI_{50} (concentration expressed in µM inhibiting 50% of cell growth or cytostatic effect) were determined through non-linear regression analysis using the concentration-response curve for each cell line in software ORIGIN 8.0® (OriginLab Corporation) [74, 75].

4.2.4 Cell treatments for Cytometry assays:

For the flow cytometry experiments, HT-29 (human colorectal adenocarcinoma, epithelial, adherent) cells were seeded in 6 well plates (2 x 10^5 cells/well) and incubated for 24 h prior to treatments.

4.2.5 Measurement of phosphatidylserine externalization

Phosphatidylserine externalization was analysed with Guava Nexin Assay Kit (Guava Technologies, Hayward, CA) in accordance with manufacturer's instructions. After 24 h, HT-29 cells were treated with **2b** (5, 20, 30 and 50 µM) for 24 h, harvested (Trypsin-EDTA 0.25%) and resuspended at a density of 1 x 10^5 cells in 100 µL of phosphate buffered saline (PBS). The binding buffer containing annexin-V-PE and 7-AAD was added to the cells (100 µL/sample) and the suspension was incubated in the dark for 20 min at room temperature. After that, cells were analyzed (5000 events/replicate) by flow cytometry (Guava Easycyte Mini – Guava Technologies, Hayward, CA).

4.2.6 Cell Cycle analyses

Cell cycle analyses were performed with the Guava Cell Cycle reagent (Guava Technologies, Hayward, CA) in accordance with manufacturer's instructions. After the first 24h, HT-29 cells were deprived of FBS for 24 h (cell cycle synchronization). After that, cells were treated with **2b** (5, 10 and 30 µM) and Colchicine (1.25 nM) for 24 h, harvested (Trypsin-EDTA 0.25%) and resuspended at a density of 1 x 10^5 cells in 100

µL of PBS. The binding buffer containing propidium iodide (PI) was added to the cells (100 µL) and suspension was incubated in the dark for 20 min at room temperature. Finally, cells were analyzed (5000 events/replicate) by flow cytometry (Guava Easycyte Mini).

4.2.7 DNA interaction

4.2.7.1 Preparation of the ct-DNA solution

Calf thymus DNA (ctDNA) was purchased from Sigma and was used without further purification. The solution of ctDNA in Tris-HCl (0,01 M, pH 7.6) buffer was sonicated for 5 min and the DNA concentration was determined using the molar extinction coefficients 6600 M^{-1} cm^{-1} at 260 nm [76]. The purity of DNA was determined by monitoring the rate value of A260/A280. DNA concentration was expressed as micromolar equivalents of the base pairs.

4.2.7.2 UV-vis absorption measurements

The derivative 2b was dissolved in DMSO at a concentration of 1 mM (stock solution) from which the working solutions were prepared by dilution using Tris-HCl (0.01 M, pH 7.6) buffer at concentrations ranging from 10 to 80 µM.

Under optimized concentration, the compounds were titrated with increasing concentrations of ctDNA. Before the measurements, the system was stirred and incubated at room temperature for 10 minutes. The measurements were performed in a rectangular quartz cuvette with a path length of 1cm.

The intrinsic binding constant (Kb) was obtained by fitting the data to equation 1 [46]:

$$[DNA]/(\varepsilon_a - \varepsilon_f) = [DNA]/(\varepsilon_b - \varepsilon_f) + 1 / Kb\ (\varepsilon_b - \varepsilon f) \quad (1)$$

where, εa; εb and εf are the apparent, bound, and free extinction coefficients, respectively. Plot fitting of $[DNA]/(\varepsilon_a - \varepsilon_f)$ vs. [DNA] used Kb obtained from the ratio of the slope to the Y intercept. The binding data were fitted using a SigmaPlot 10.0 software.

4.2.7.3 Fluorescence Measurements

Fluorescence measurements of non-bound derivative were performed with 15 µM of compound 2b in 0.01 M Tris buffer, pH 7.6. Emission spectra were recorded in the region 370-700 nm using an excitation wavelength of 220-400 nm. All

measurements were performed at 25 °C in a rectangular quartz cuvette with a 1 cm path length. Fluorescence intensities were expressed in arbitrary units. Fluorescence titrations were conducted by the addition of increasing amounts of ctDNA directly into the cell containing the derivatives.

The behavior suppression emission was analyzed by the Stern-Volmer equation was obtained through the equation (2) [62]:

$$F_0 / F = 1 + K_{SV} [Q] \quad (2)$$

where, F_0 and F are the fluorescence intensities in the absence and presence of indoles derivatives. K_{SV} is the constant linear suppression. [Q] is the concentration of derivatives. The plot of relative emission intensity (F_0/F) versus [Q] was used to obtain the constant from the linear regression. The binding data were fitted using a SigmaPlot 10.0 software.

4.2.8 *In vitro* topoisomerase II inhibition assay

Human topoisomerase IIα inhibition activity was determined as previously described by Almeida et al. (2016) [70]. Briefly, 100 ng pUC19 DNA plasmid (from Sigma) and 4.0 unit of recombinant human (p170) topoisomerase II (Sigma-Aldrich) in relaxation buffer without or with 2b or amsacrine (*m*-AMSA) were incubated for 30 min at 37º C. The tested concentrations were 50 and 100 µM. Reactions were terminated with 1% SDS and digested with proteinase K. Then, the reaction products were analyzed by electrophoresis gel stained with Ethidium Bromide and photographed under UV light.

4.2.9 Statistical analyses

The results were expressed as the mean ± standard error and by analysis of variance (ANOVA), one-way followed by Tukey tests. P values lower than 0.05 ($p<0.05$) were considered as indicative of significance and represented by: *$p<0.05$, **$p<0.01$ and ***$p<0.001$. The calculations were performed using the statistical software GraphPad Prism version 7.0, San Diego California, USA.

Acknowledgements

This study was supported by Brazilian agencies Fundação de Amparo Pesquisa do Estado de Pernambuco (FACEPE, Brazil) and Conselho Nacional de Desenvolvimento Científico e Tecnológico (CNPq).

Conflict of Interest

The authors declare that there was no competing interests.

References

[1] Globocan. Cancer Incidence and Mortality Worldwide: IARC Cancer Base No. 11 [Internet]. Lyon, France: International Agency for Research on Cancer; 2013: http://globocan.iarc.fr. (accessed: November 2016).

[2] N. Bailón-Moscoso, J.C. Romero-Benavides, P. Ostrosky-Wegman, Development of anticancer drugs based on the hallmarks of tumor cells, Tumor Biol. 35 (2014) 3981-3995.

[3] M. Sirajuddin, S. Ali, A. Badshah, Drug-DNA interactions and their study by UV-Visible, fluorescence spectroscopies and cyclic voltammetry, J Photochem Photobiol B. 124 (2013) 1-19.

[4] M.M. Aleksic, V. Kapetanovic, An overview of the optical and electrochemical methods for detection of DNA-drug interactions, Acta Chim Slov. 61 (2014) 555-573.

[5] Y. Pommier, E. Kiselev, C. Marchand, Interfacial inhibitors, Bioorganic & Medicinal Chemistry Letters 25 (2015) 3961-3965.

[6] Y. Pommier, E. Leo, H. Zhang, C. Marchand, DNA topoisomerases and their poisoning by anticancer and antibacterial drugs, ACS Chem Biol. 17 (2010) 421-433.

[7] M.K. Kathiravan, M.M. Khilare, K. Nikoomanesh, A.S. Chothe, K.S. Jain, Topoisomerase as target for antibacterial and anticancer drug discovery, J Enzyme Inhib Med Chem. 28 (2013) 419-435.

[8] J.L. Nitiss, Targeting DNA topoisomerase II in cancer chemotherapy, Nat Rev Cancer. 9 (2009) 338-350.

[9] O. Sordet, S. Solier, Topoisomerases and Apoptosis, in: Y. Pommier (Ed.), DNA Topoisomerases and Cancer, Springer, New York, 2012.

[10] S. Arora, S. Agarwal, S. Singhal, Anticancer activities of thiosemicarbazides/thiosemicarbazones: A review, J Pharm Pharm Sci. 9 (2014) 34-41.

[11] N. Sharma, D.P. Pathak, Combatting challenging aspects of cancer with thiosemicarbazones, J Pharm Pharm Sci. 8 (2016) 27-34.

[12] J.F. Oliveira, A.L. Silva, D.B. Vendramini-Costa, C.A.C. Amorim, J.F. Campos, A. G. Ribeiro, R.O. Moura, J.L. Neves, A.L.T.G. Ruiz, J.E. Carvalho, M.C.A. Lima,

Synthesis of thiophene-thiosemicarbazone derivatives and evaluation of their in vitro and in vivo antitumor activities, Eur J Med Chem. 104 (2015) 148-156.

[13] S. Krishan, D.R. Richardson, S. Sahni, The Anticancer Agent, Di-2-Pyridylketone 4,4-Dimethyl-3-Thiosemicarbazone (Dp44mT), Up-Regulates the AMPK-Dependent Energy Homeostasis Pathway in Cancer Cells, Biochim Biophys Acta. 1863 (2016) 2916-2933.

[14] S.M.V. Almeida, E.A. Lafayette, L.B.P.G. Silva, C.A.C. Amorim, T.B. Oliveira, A.L.T.G. Ruiz, J.E. Carvalho, R.O. Moura, E.I.C. Beltrão, M.C.A. Lima, L.B. Carvalho-Júnior, Synthesis, DNA binding, and Antiproliferative activity of novel acridine-thiosemicarbazone derivatives, Int J Mol Sci. 16 (2015) 13023-13042.

[15] A.M. Merlot, N.H. Shafie, Y. Yu, V. Richardson, P.J. Jansson, S. Sahni, D.J. Lane, Z. Kovacevic, D.S. Kalinowski, D.R. Richardson, Mechanism of the induction of endoplasmic reticulum stress by the anti-cancer agent, di-2-pyridylketone 4,4-dimethyl-3-thiosemicarbazone (Dp44mT): Activation of PERK/eIF2α, IRE1α, ATF6 and calmodulin kinase, Biochem Pharmacol. 109 (2016) 27-47.

[16] H. Huang, Q.Chen, X. Ku, L. Meng, L. Lin, X. Wang, C. Zhu, Y. Wang, Z. Chen, M. Li, H. Jiang, K. Chen, J. Ding, H. Liu, A series of alpha-heterocyclic carboxaldehyde thiosemicarbazones inhibit topoisomerase IIalpha catalytic activity, J Med Chem., 53 (2010) 3048-3064.

[17] C. Zhang, Y. Qu, B. Niu, Design, synthesis and biological evaluation of lapachol derivatives possessing indole scaffolds as topoisomerase I inhibitors, Bioorg Med Chem. 24 (2016) 5781-5786.

[18] J. Yan, J. Hu, B. An, L. Huang, X. Li, Design, synthesis, and biological evaluation of cyclic-indole derivatives as anti-tumor agents via the inhibition of tubulin polymerization, Eur J Med Chem. 125 (2016) 663-675.

[19] P.M. Kelly, S.A. Bright, D. Fayne, J.K. Pollock, D.M. Zisterer, D.C. Williams, M.J. Meegan, Synthesis, antiproliferative and pro-apoptotic activity of 2-phenylindoles, Bioorg Med Chem. 24 (2016) 4075-4099.

[20] R. Ottana, R. Maccari, M.L. Barreca, G. Bruno, A. Rotondo, A. Rossi, G. Chiricosta, R. Di Paola, L. Sautebin, S. Cuzzocread, M.G. Vigorita, 5-Arylidene-2-imino-4-thiazolidinones: Design and Synthesis of Novel Anti-inflammatory Agents, Bioorg Med Chem. 13 (2005) 4243-4252.

[21] T.M. Aquino, A.P. Liesen, I. Spacov, C.S. Carvalho, V.T. Lima, A. Alves, A.R. Faria, J.M. Araujo, J.G. Lima, E.J.T. Melo, A.J.S. Góes, Synthesis, Anti-Toxoplasma gondii and Antimicrobial Activities of 2-Hydrazolyl-3-phenyl-5-(4-nitrobenzylidene)-4-thiazolidinone Substituted Derivatives, Lat Am J Pharm. 30 (2011) 1567-1573.

[22] N. Bharti, Shailendra, S. Sharma, F. Naqvi, A. Azam, New palladium (II) complexes of 5-nitrothiophene-2-carboxaldehyde thiosemicarbazones: Synthesis, spectral studies and *in vitro* anti-amoebic activity, Bioorg Med Chem. 11 (2003) 2923-2929.

[23] I. Antonini, F. Claudi, P. Franchetti, M. Grifantini, S. Marteli, Elucidation of the structure of the antineoplastic agents, 2-formylpyridine and 1-formylisoquinoline thiosemicarbazones, J Med Chem. 20 (1977) 447-449.

[24] Z. El-Gendy, R.M. Abel-Rahman, M.M. Fawzy, M.B. Mahmoud, Biologically active thiazolidinone. Part II. Synthesis and fungitoxicities of isolated and fused thiazolidinones derived from thiosemicarbazones. J Indian Chem Soc. 67 (1990) 927-929.

[25] N. Ulusoy, M. Kiraz, O. Kuçukbasmaci, New 6-(4-Bromophenyl)-imidazo[2,1-*b*]thiazole Derivatives: Synthesis and Antimicrobial Activity, Monatsh Chem. 133 (2002) 1305-1315.

[26] N. Ergenç, G. Capan, N.S. Gunay, S. Ozkirimli, M. Gungor, S. Ozbey, E. Kendi, Synthesis and hypnotic activity of new 4-thiazolidinone and 2-thioxo-4,5-imidazolidinedione derivatives, Arch Pharm (Weinheim). 332 (1999) 343-347.

[27] R. Pingaew, S. Prachayasittikul, S. Ruchirawat, V. Prachayasittikul, Synthesis and cytotoxicity of novel N-sulfonyl-1,2,3,4-tetrahydroisoquinoline thiosemicarbazone derivatives, Med Chem Res. 22 (2013) 267-277.

[28] I. Dilovic, M. Rubcic, V. Vrdoljak, S.K. Pavelic, M. Kralj, I. Piantanida, M. Cindric, Novel thiosemicarbazone derivatives as potential antitumor agents: synthesis, physicochemical and structural properties, DNA interactions and antiproliferative activity, Bioorg Med Chem. 16 (2008) 5189-5198.

[29] N. Ergenç, G. Capan, Synthesis and anticonvulsant activity of new 4- thiazolidone and 4-thiazoline derivatives, Farmaco. 49 (1994) 133-135.

[30] Z. Afrasiabi, E. Sinn, J. Chen, Y. Ma, A.L. Rheingold, L.N. Zakharov, N. Rath, S. Padhye, Appended 1,2-naphthoquinones as anticancer agents 1: synthesis, structural, spectral and antitumor activities of ortho-naphthaquinone thiosemicarbazone and its transition metal complexes, Inorg Chim Acta. 357 (2004) 271-278.

[31] J. Chen, Y.W. Huang, G. Liu, Z. Afrasiabi, E. Sinn, S. Padhye, Y. Ma, The cytotoxicity and mechanisms of 1,2-naphthoquinone thiosemicarbazone and its metal derivatives against MCF-7 human breast cancer cells, Toxicol Appl Pharmacol. 197 (2004) 40-48.

[32] G.J. Karabatsos, F.M. Vane, R.A. Taller, N. Hsi, Structural studies by nuclear magnetic resonance. VIII. Ring-substituted phenylhydrazones, semicarbazones and thiosemicarbazones, J Am Chem Soc. 86 (1964) 3351-3358.

[33] Z. Liu, S. Wu, Y. Wang, R. Li, J. Wang, L. Wang, Y. Zhao, P. Gong, Design, synthesis and biological evaluation of novel thieno[3,2-d] pyrimidine derivatives possessing diaryl semicarbazone scaffolds as potent antitumor agentes, Eur J Med Chem. 87 (2014) 782-793.

[34] M.R. Boyd, K.D. Paull, Some practical considerations and applications of the National Cancer Institute in vitro anticancer drug discovery screen, Drug Dev Res. 34 (1995) 91-109.

[35] P. Skehan, R. Storeng, D. Scudiero, A. Monks, J. McMahon, D. Vistica, J.T. Warren, H. Bokesch, M.R. Boyd, New colorimetric cytotoxicity assay for anticancer-drug screening, J Natl Cancer Inst. 82 (1990) 1107-1112.

[36] G. Fouche, G.M. Cragg, P. Pillay, N. Kolesnikova, V.J. Maharaj, J. Senabe, In vitro anticancer screening of South African plants, J Ethnopharmacol. 119 (2008) 455-461.

[37] R.B. Ravelli, B. Gigant, P.A. Curmi, I. Jourdain, S. Lachkar, A. Sobel, M. Knossow, Insight into tubulin regulation from a complex with colchicine and a stathmin-like domain, Nature. 428 (2004) 198-202.

[38] M.A. Jordan, L. Wilson, Microtubules as a target for anticancer drugs, Nat Rev Cancer. 4 (2004) 253-65.

[39] D. Hanahan, R.A. Weinberg, Hallmarks of cancer: the next generation, Cell. 144 (2011) 646-74.

[40] S. Sarkar, P. Bhattacharjee, K. Bhadra, DNA binding and apoptotic induction ability of harmalol in HepG2: Biophysical and biochemical approaches, Chem Biol Interact. 258 (2016) 142-152.

[41] J. Carvalho, P. Nottelet, J.L. Mergny, J.A. Queiroz, G.F. Salgado, C. Cruz, Study of the interaction between indole-based compounds and biologically relevant G-quadruplexes, 135 (2017) 186-195.

[42] H. Ihmels, D. Otto, Intercalation of organic dye molecules intodouble-stranded DNA general principles and recent developments, Top Curr Chem (J). 258 (2005) 161-204.

[43] E.A. Lafayette, S.M.V. Almeida, M.G.R. Pitta, E.I.C. Beltrão, T.G. Silva, R.O. Moura, I.R. Pitta, L.B. Carvalho-Júnior, M.C.A. Lima, Synthesis, DNA binding and topoisomerase I inhibition activity of thiazacridine and imidazacridine derivatives, Molecules. 18 (2013) 15035-15050.

[44] Q. Wang, W. Li, A. Liu, B. Zhang, F. Gao, S. Li, X. Liao, Binding and photocleavage of a neutral nickel (II) bis(hydrogen pyridine-2,6-dicarboxylate) complex DNA, J Mol Struct. 985 (2011) 129-133.

[45] S. Kashanian, E.N. Dolatabadi, DNA binding studies of 2-tert-butylhydroquinone (TBHQ) food additive, Food Chem. 116 (2009) 743-747.

[46] J.D. McGhee, P.H. Von Hippel, Theoretical aspects of DNA-Protein interactions: Co-operative and non-co-operative binding of larg ligands to a one-dimensional homogeneous lattice, J Mol Biol. 86 (1974) 469-489.

[47] D.K. Jangir, S.K. Dey, S. Kundu, K. Mehrotra, Assessment of amsacrine bindingwith DNA using UV-visible, circular dichroism and Raman spectroscopictechniques, J Photochem Photobiol B. 114 (2012) 38-43.

[48] M.F. Hassan, A. Rauf, Synthesis and multi-spectroscopic DNA binding study of 1,3,4-oxadiazole and 1,3,4-thiadiazol derivatives of fatty acid, Spectrochim Acta A Mol Biomol Spectrosc. 153 (2016) 510-516.

[49] P. Pakravan, S. Masoudian, Study on the Interaction between Isatin-*β*-Thiosemicarbazone and Calf Thymus DNA by Spectroscopic Techniques, Iran J Pharm Res. 14 (2015) 111-123.

[50] K. Benner, H. Ihmels, S. Kolsch, P.M. Pithan, Targeting abasic site-containing DNA with annelated quinolizium derivatives: the influence of size, shape and substituents, Org Biomol Chem. 12 (2014) 1725-1734.

[51] S. Janardan, P. Suman, G. Swapna, A. Amrita, R. Priya, R. Siva, K. Vijayakrishna, A. Sivaramakrishna, Evaluation of DNA Binding with Some Selected Hydrazide and Semicarbazide Derivatives, Appl Biochem Biotechnol. 173 (2014) 596-608.

[52] S. Kurbanoglu, B. Dogan-Topal, E.V. Rodriguez, B. Bozal-Palabiyik, S.A. Ozkan, B. Uslu, Advances in electrochemical DNA biosensors and their interaction mechanism with pharmaceuticals, J Electroanal Chem (Lausanne). 775 (2016) 9-26.

[53] A. Ali, S. Bhattacharya, DNA binders in clinical trials and chemotherapy, Bioorg Med Chem. 22 (2014) 4506-4521.

[54] A. Rescifina, C. Zagni, M.G. Varrica, V. Pistara, A. Corsaro, Recent advances in small organic molecules as DNA intercalating agents: synthesis, activity and modeling, Eur J Med Chem. 74 (2014) 95-115.

[55] S. Geng, Y. Cui, Q. Liu, F. Cui, G. Zhang, Y. Chi, H. Peng, Spectroscopic and molecular modeling study on the interaction of ctDNA qith 3'-deoxy-3'-azido doxorubicin, J Lumin. 141 (2013) 144-149.

[56] S. Bi, L. Yan, Y. Wang, B. Pang, T. Wang, Spectroscopic study on the interaction of eugenol with salmon sperm DNA in vitro, J Lumin. 132 (2012) 2355-2360.

[57] H. Joshi, A. Sengupta, K. Gavyala, P. Hazra, Unraveling the mode of binding of the anticancer drug topotecan with dsDNA, RSC Adv. 4 (2014) 1015-1024.

[58] S.S. Mati, S.S. Roy, S. Chall, S. Bhattacharya, S.B. Chandra, Unveiling the Groove Binding Mechanism of a Biocompatible Naphthalimide-Based Organoselenocyanate with Calf Thymus DNA: An “Ex Vivo” Fluorescence Imaging Application Appended by Biophysical Experiments and Molecular Docking Simulations, J Phys Chem B. 117 (2013) 14655-14665.

[59] B.K. Paul, N. Guchhait, Exploring the Strength, Mode, Dynamics, and Kinetics of Binding Interaction of a Cationic Biological Photosensitizer with DNA: Implication on

Dissociation of the Drug–DNA Complex via Detergent Sequestration, J Phys Chem B. 115 (2011) 11938-11949.

[60] Y. Lu, J. Lv, G. Zhang, G. Wang, Q. Liu, Interaction of an anthracycline disaccharide with ctDNA: Investigation by spectroscopic technique and modeling studies, Spectrochim Acta A Mol Biomol Spectrosc. 75 (2010) 1511-1515.

[61] F. Cui, R. Huo, G. Hui, X. Lv, J. Jin, G. Zhang, W. Zing, Study on the interaction between aglycon of daunorubicin and calf thymus DNA by spectroscopy, J Mol Struct. 1001 (2011) 104-110.

[62] J.R. Lakowicz, Principles of Fluorescence Spectroscopy, Third ed., Springer, 2006.

[63] C. Gao, F. Liu, X. Luan, C. Tan, H. Liu, Y. Xie, Y. Jin, Y. Jiang, Novel synthetic 2-amino-10-(3,5-dimethoxy)benzyl-9(10H)-acridinone derivatives as potent DNA-binding antiproliferative agents, Bioorg Med Chem. 18 (2010) 7507-7514.

[64] F. Cui, Q. Liu, H. Luo, G. Zhang, Spectroscopic, viscosity and molecular modeling studies on the interaction of 3'-azido-danorubicin thiosemicarbazone with DNA, J Fluoresc. 24 (2014) 189-195.

[65] J. Nateewattana, S. Dutta, S. Reabroi, R. Saeeng, S. Kasemsook, A. Chairoungdua, J. Weerachayaphorn,S. Wongkham, P. Piyachaturawat, Induction of apoptosis in cholangiocarcinoma by an andrographolide analogue is mediated through topoisomerase II alpha inhibition, European Journal of Pharmacology 723 (2014) 148-155.

[66] J.C. Yalowich, X. Wuc, R. Zhang, R. Kanagasabai, M. Hornbaker, B.B. Hasinoff, The anticancer thiosemicarbazones Dp44mT and triapine lack inhibitory effects as catalytic inhibitors or poisons of DNA topoisomerase IIa, Biochem Pharmacol. 84 (2012) 52-58.

[67] A.M. Azarova, Y.L. Lyu, C.P. Lin, Y.C. Tsai, J.Y. Lau, J.C. Wang, L.F. Liu, Roles of DNA topoisomerase II isozymes in chemotheraphy and secondary malignancies, Proc Natl Acad Sci U.S.A. 104 (2007) 11014-11019.

[68] H. Huang, Q. Chen, X. Ku, L. Meng, L. Lin, X. Wang, C. Zhu, Y. Wang, Z. Chen, M. Li, H. Jiang, K. Chen, J. Ding, H. Liu, A Series of α-Heterocyclic Carboxaldehyde Thiosemicarbazones Inhibit Topoisomerase IIα Catalytic Activity, J Med Chem. 53 (2010) 3048-3064.

[69] M.K. Kathiravan, A.N. Kale, S. Nilewar, Discovery and Development of Topoisomerase Inhibitors as Anticancer Agents, Mini Rev. Med. Chem. 16 (2016) 1219-1229.

[70] S.M. Almeida, E.A. Lafayette, W.L. Silva, V.L. Serafim, T.M. Menezes, J.L. Neves, A.L. Ruiz, J.E. Carvalho, R.O. Moura, E.I. Beltrão, L.B. Carvalho-Júnior, M.D. Lima, New spiro-acridines: DNA interaction, antiproliferative activity and inhibition of human DNA topoisomerases, Int J Biol Macromol. 92 (2016) 467-475.

[71] J. Chen, J. Huang, G. Liu, Z. Afrasiabi, E. Sinn, S. Padhye, Y. Ma, The cytotoxicity and mechanisms of 1,2-naphthoquinone thiosemicarbazone and its metal derivatives against MCF-7 human breast cancer cells, Toxicol Appl Pharmacol. 197 (2004) 40-48.

[72] M. Kashyap, S. Kandekar, A.T. Baviskar, D. Das, R. Preet, P. Mohapatra, S.R. Satapathy, S. Siddharth, S.K. Guchhait, C.N. Kundu, U.C. Banerjee, Indenoindolone derivatives as topoisomerase II-inhibiting anticancer agents, Bioorg Med Chem Lett. 23 (2013) 934-938.

[73] N. Bucher, G2 checkpoint abrogation and checkpoint kinase-1 targeting in the treatment of cancer, Br J Cancer. 98 (2008) 523-528.

[74] A. Monks, D. Scudiero, P. Skehan, R. Shoemaker, K. Paull, D. Vistica, C. Hose, J. Langley, P. Cronise, A. Vaigro-Wolff, M. Gray-Goodrich, H. Campbell, J. Mayo, M. Boyd, Feasibility of a high-flux anticancer drug screen using a diverse panel of cultured human tumor cell lines, J Natl Cancer Inst. 83 (1991) 757.

[75] R. Shoemaker, The NCI60 human tumour cell line anticancer drug screen, Nat Rev Cancer. 6 (2006) 813.

[76] A. Wolfe, G.H. Shimer-Jr, T. Meehan, Polycyclic aromatic hydrocarbons physically intercalate into duplex regions of denatured DNA, Biochemistry. 26 (1987) 6392-6396.

Table 1. *In vitro* antiproliferative activity (GI_{50}[a] in µM) of thiosemicarbazones and 4-thiazolidinones based-indole derivatives

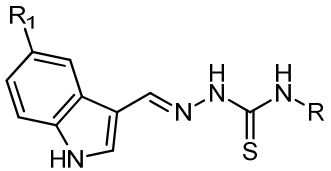

2a-e

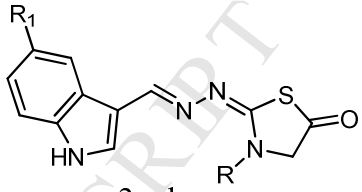

3a-d

Cell Lines	2a R = 1-naphtyl R_1 = Br	2b R = 1-naphtyl R_1 = H	2c R = p-toluyl R_1 = H	2d R = 2-phenethyl R_1 = Br	2e R = 2-phenethyl R_1 = H	3a R = 1-naphtyl R_1 = Br	3b R = 1-naphtyl R_1 = H	3c R = p-toluyl R_1 = Br	3d R = p-toluyl R_1 = H	Dox
U251	7.32	0.92	8.11	7.49	77.90	48.81	72.52	54.71	90.16	0.14
MCF 7	0.95	0.25	2.52	6.81	15.54	6.06	34.88	59.52	>100	0.07
NCI-ADR/RES	6.18	6.48	1.46	7.14	38.74	12.41	38.57	64.58	>100	0.77
786-0	6.56	0.25	3.99	7.58	76.29	29.09	62.08	39.85	79.14	0.11
NCI-H460	6.99	0.38	11.72	8.48	>100	>100	>100	96.60	>100	0.09
OVCAR-3	1.60	0.21	3.88	8.22	>100	5.12	25.74	98.50	>100	0.22
HT29	6.56	0.01	1.45	7.87	>100	27.34	96.86	>100	>100	0.23
K562	5.29	0.01	0.16	2.12	0.17	>100	>100	0.01	>100	0.93
mean log GI_{50}	0.63 M	-0.69 P	0.39 M	0.81 M	>1.47 I	>1.40 I	>1.77 I	>1.36 I	>1.98 I	-0.68 P
HaCat	6.15	0.59	0.99	7.85	>100	6.23	62.98	54.00	>100	0.20

[a] GI_{50} = concentration (µM) that inhibits cell growth by 50% after 48 h exposition; GI_{50} was determined from nonlinear regression analyses by using ORIGIN 8.0 software (OriginLab Corporation). Experiments conducted in triplicate. Dox: doxorubicine, positive control.
Classification criteria: inactive (I, mean log GI50 > 1.50), weak activity (W, 1.50 > log GI50 > 1.10), moderate activity (M, 1.10 > mean log GI50 > 0) and potent activity (P, mean log GI50 < 0) (Fouche et al., 2008).

Table 2. Influence of **2b** on HT29 cells cycle after 24h-exposition

Treatments		Sub-G1	G1	S	G2/M
Vehicle		3.5 ± 0.7	46.1 ± 2.1	17.2 ± 1.2	32.5 ± 2.3
Colchicine	1.25 nM	3.5 ± 0.6	14.6 ± 1.8***	5.9 ± 1.3***	76.0 ± 1.7***
	5 µM	2.0 ± 0.5	10.7 ± 0.8***	6.8 ± 1.4***	80.5 ± 2.4***
2b	10 µM	1.6 ± 0.3	26.7 ± 1.3***	5.5 ± 0.4**	66.2 ± 1.2***
	30 µM	4.8 ± 0.8	34.9 ± 1.4***	7.3 ± 0.8***	53.1 ± 1.3***

Distribution of cells in the different phases of cell cycle, after 24 h of treatment with (DMSO 0.1%), Colchicine (1.25 nM) and derivative 2b (5, 10 and 30 µM). Mean (%) ± standard error of two independent experiments in triplicate. A total of 5000 events were collected per experiment. ANOVA followed by Tukey's Multiple Comparison Test. **p < 0.01, ***p < 0.001, statistically different from vehicle.

Table 3. UV-Vis absorption and fluorescence emission data of derivative **2b** in the absence and presence of ctDNA.

	λ_{max}							
Compound	Free	Bound	**Extinction Coefficient (ε) M^{-1}**	**Hyperchr.[a]**	**Hyperchr.[a]**	**λ excitation**	**λ emission**	**K_{sv} M^{-1}**
2b	334 nm	334 nm	18.440	13%	4.3×10^4	335 nm	435 nm	1.19×10^3

[a]Hyperchromicity for complexes formed by compound 2b and 100 µM of ctDNA in comparison to free ligands.

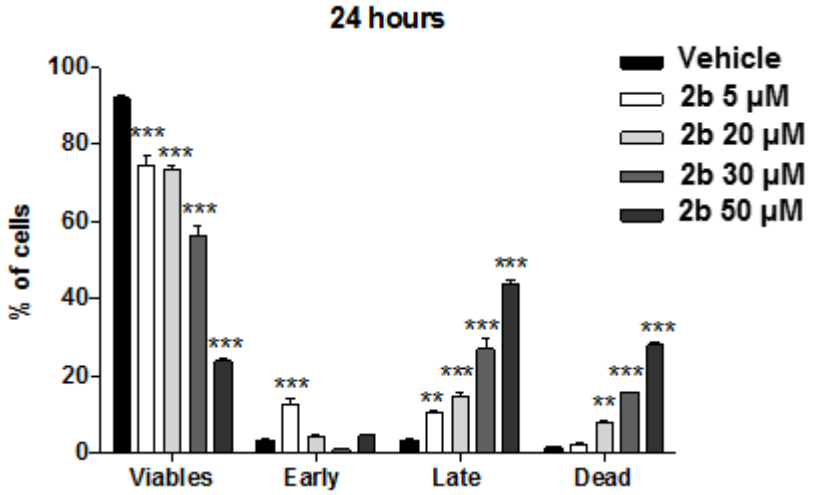

Figure 1. Compound 2b induces cell death in HT-29 cells. Cells were treated for 24 h with vehicle (DMSO 0.1%) and compound 2b (5, 20, 30 and 50 µM). Results are expressed as mean ± standard error from two independent experiments in triplicate, in percentage of cells stained with annexin-V only (early cell death), double stained with annexin-V and 7-AAD (late cell death), stained with 7-AAD only (dead cells or cellular debris) and unstained (viable cells). A total of 5000 events were collected per experiment. ANOVA followed by Tukey's Multiple Comparison Test. **p < 0.01, ***p < 0.001, statistically different from vehicle.

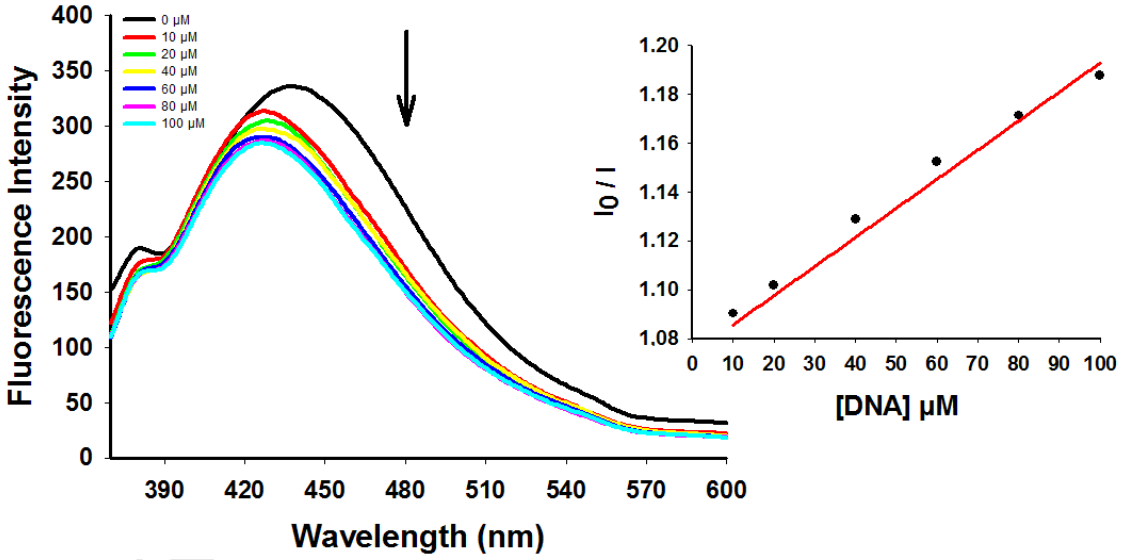

Figure 2. Fluorescence spectra of derivative 2b (15 µM) with increasing concentration of ctDNA. Insert: corresponding the fluorescence intensity of bound derivative to ctDNA.

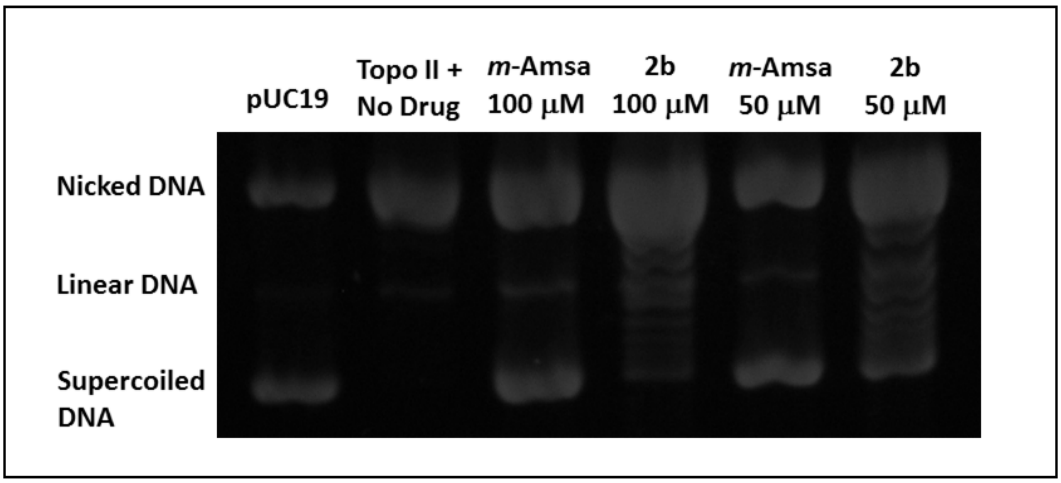

Figure 3. Effect of derivative 2b on inhibition of Topo IIα. Inhibition of TopoIIα-induced DNA relaxation by derivative 2b and *m*-AMSA as positive control. Native supercoiled pUC19 was incubated for 30 min at 37 °C with 4 units of human Topo IIα in the absence or presence of ligands at concentrations of 50 and 100 µM.

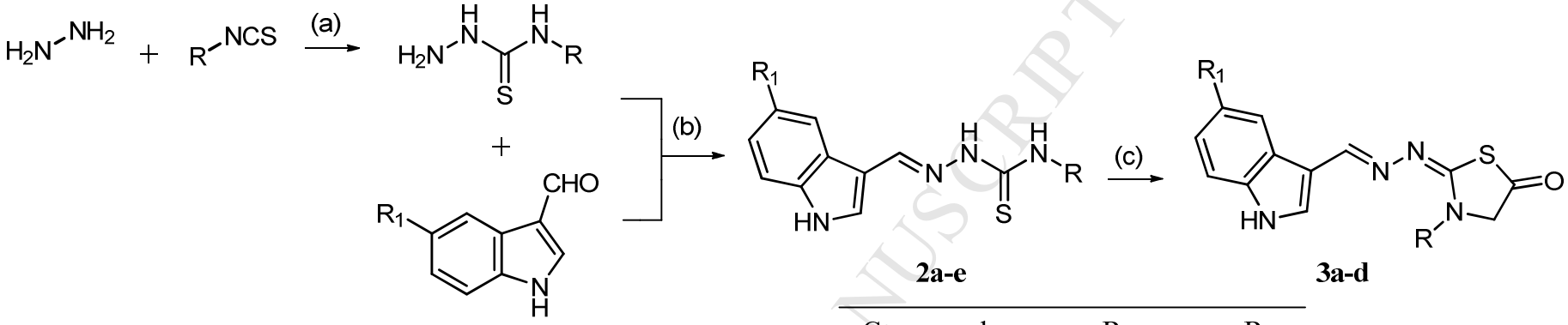

2a-e **3a-d**

Compound	R	R_1
2a	1-naphtyl	Br
2b	1-naphtyl	H
2c	p-tolyl	H
2d	2-phenetyl	Br
2e	2-pheneyl	H
3a	1-naphtyl	Br
3b	1-naphtyl	H
3c	p-tolyl	Br
3d	p-tolyl	H

Scheme 1. Synthesis of thiosemicarbazones (2a-e) and 4-thiazolidinone (3a-d) derivatives. Reagents and conditions: (a) $CHCl_2$, room temperature; (b) AcOH (few drops), EtOH, room temperature; (c) $ClCH_2COOEt$, sodium acetate, EtOH, reflux.

Highlights

- ✓ Compound **2b** was the most promising especially against colorectal adenocarcinoma (HT-29) cell;
- ✓ Compound **2b** induced phosphatidylserine residues exposition and G2/M arrest on HT-29 cells;
- ✓ Compound **2b** was able to interact with ctDNA and inhibited topoisomerase IIα activity.